# Design and Analysis of a 6-DOF Haptic Device for Teleoperation Using a Singularity-Free Parallel Mechanism

**Tawee Ngamvilaikorn and Viboon Sangveraphunsiri**
Robotics and Manufacturing Lab. Department of Mechanical Engineering
Faculty of Engineering, Chulalongkorn University,
Bangkok 10330, Thailand
Viboon.s@eng.chula.ac.th

## Abstract

This work concerns the design and development of a six degrees of freedom haptic device. The haptic device is used as the master arm for internet-based teleoperation purposes. For the experimentation, the Stewart platform, the other parallel mechanism, is used as the slave arm. The force reflex from the slave arm is transmitted to the operator through the Tendon-Pulley train of the master arm. Virtual guidance can be implemented in the master arm to improve the maneuverability for the operators. Low inertia, friction force, and backlash are minimized in the design. Singularity is also eliminated. The inverse and forward kinematics as well as the Jacobian of the master arm are derived. The closed-form solution of the forward kinematics can be obtained by installing 9 encoders, instead of 6. The end-point of the master arm is sent to the slave arm as commands. The slave arm transforms the commands to joint variables by using the inverse kinematics of the slave arm. The experimental results show that the haptic device is capable of controlling the Stewart platform and can be used for other parallel mechanisms as well.

**Keywords:** Haptic, Teleoperation, Parallel Mechanism, Virtual Wall

## 1. Introduction

Conventional robot arms are typically controlled by preprogramming of the desired paths within the robot workspace. This will limit the capability of the robot arm. There are some applications which we cannot form the desired paths at the beginning. Manual manipulation is needed to help the operator to control the manipulator arm. In this case, master-slave or teleoperation is required to fulfill the task. Besides the path following control of the teleoperation, information of the force reacting at the slave should be reflected back to the operator at the master side. This is the haptic system characteristic. In this work we developed a 6 degrees of freedom master-slave human-assisted manipulator arm with force reflected system or a 6 degrees of freedom haptic system as shown in Figure 1. We purpose a new closed-chain configuration which is a singular-free parallel mechanism. Relaxation of kinematics similarly between the master and slave is assumed. We also introduce virtual guidance to improve the maneuverability for the operators. The virtual guidance can be a desired path or a boundary of the desired workspace. Any limited control volume can also be controlled or specified by this virtual guidance technique. In this work, we will assume that there is -- significant effect due to the time delay in the internet-based teleoperation. From previous works, we developed a 6 DOF parallel mechanism based on the Stewart platform as described in [1] and Figure 1. A stable numerical solution method for forward kinematics also was explained. In [2], we developed a 6 DOF master-slave human assisted manipulator arm based on the serial mechanism as described in [2]. We illustrated a unique design of the master-arm. A tendon-pulley was used in the master arm to transmit both motion and force between operator and the manipulator arm. In [4], we developed another unique 4 DOF parallel Robot. The robots will be used as a machine for product prototyping. Other types of parallel robots were also developed by many researchers with different configurations such as Kaist Master [5], the Y-Star parallel manipulator [8], and the Agile eye [9]. Our parallel manipulator is designed so that it can be back

drive-able. This is the requirement of the haptic master-arm for a product prototyping system under development by the author. The teleoperation can be performed under an intranet environment. The ground work of internet-based teleoperation can be found in [3].

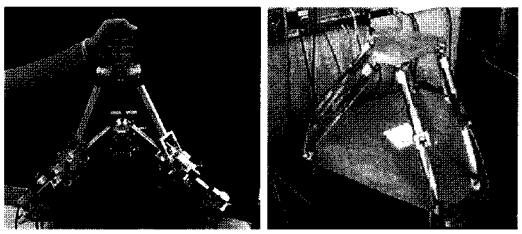

Figure 1. The 6 dof haptic system as the master and the Stewart as the slave

## 2. The Master-Slave System

Figure 1 shows the master-slave arm developed for this project. The master arm has 6 degrees of freedom with a tendon-pulley train driving mechanism. The mechanism is back drivable. The tendon-pulley system used in this mechanism has the same functions as the pulley-belt with fixed or variable distance between the two unparallel rotating axes. As shown in Figure 2, frame B and frame M are the center of the based frame and upper base, respectively. Revolute joint 1 and Prismatic joint, formed as sliding-rotating link, shown in Figure 2, are controlled by a DC servomotor. Revolute joint 2 is a passive joint with a rotary encoder attached.

### Forward Kinematics

We develop a unique design of the tendon-pulley system which supports decoupled motion of translation and rotation within the same driving mechanism.

From figure 3, for each link, $i$ = 1, 2, 3, the $r_b$ represents the distance between the center of the base (frame 0 or frame B) and center of the link or the origin of the link coordinate frame (frame i), $d^i$ represents the distance of the sliding joint of link i, and $L^i$ is the length of link i as shown in the figure. ( $L^1 = L^2 = L^3 = L$ ). The angles between the line joining the origin of the base to the origin of the link and x-axis are $\theta_1^1 = 0°$, $\theta_1^2 = 120°$, $\theta_1^3 = 240°$. The angle of the slide link with y-axis can be written as $\theta_2^1 = \theta_2^2 = \theta_2^3 = 60°$. We will define that $c\bullet = \cos(\bullet)$ and $s\bullet = \sin(\bullet)$. From Figure 3, the forward kinematics can be derived starting for the base frame (frame 0 or frame B), frame 1: the origin of the prismatic joint and frame 2: the origin of the sliding joint which moves in the direction of the prismatic joint. The origin of frame 3 and frame 4 are located at the same position of the origin of frame 2 and attached to rotating joints 1 and 2 respectively, as illustrated in Figures 2 and 3. Frame 5 is attached to the spherical joint at a corner of the upper base. Figure 3 shows the configuration of all the coordinate system. The homogeneous transformation of the coordinate frame j+1 to the coordinate frame j of link i can be written as:

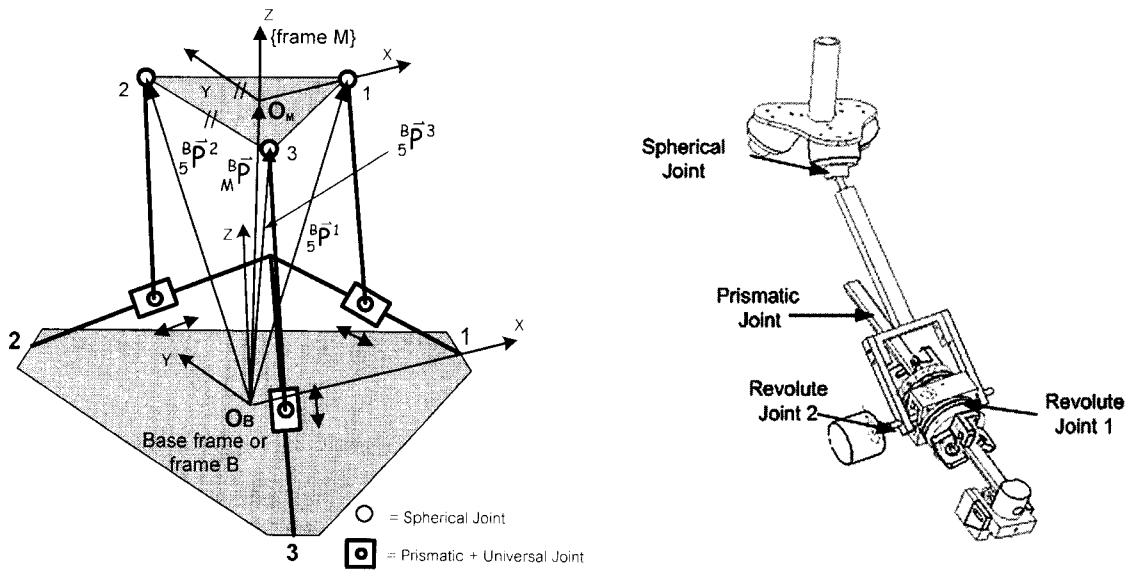


**Figure 2** Define the position vector of each joint 5 with respect to the base frame and illustrate the Tendon-Pulley system of the sliding-rotating link of each link

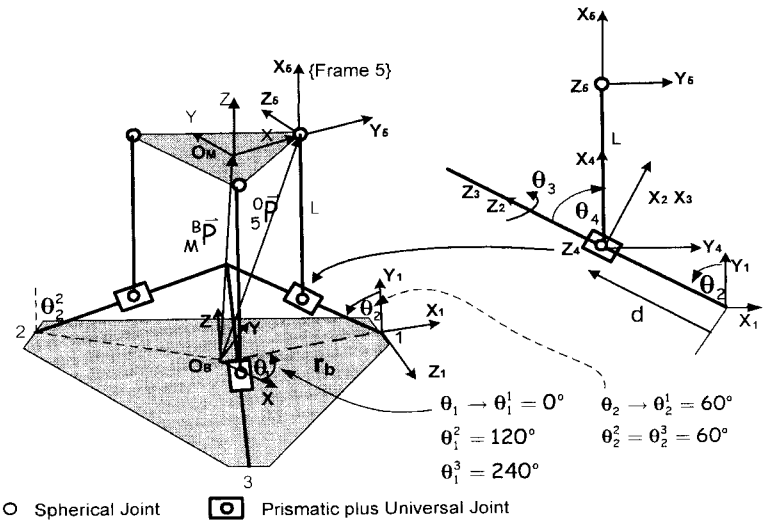


**Figure 3** The configuration of the coordinate frame of the haptic arm coordinate frame j of link i can be written as :

( $j = 0,1,2,3,4$ and frame 0 is frame B)

$$ {}^{B}_{1}T^{i} = \begin{bmatrix} c\theta_1^i & 0 & s\theta_1^i & r_b c\theta_1^i \\ s\theta_1^i & 0 & -c\theta_1^i & r_b s\theta_1^i \\ 0 & 1 & 0 & 0 \\ 0 & 0 & 0 & 1 \end{bmatrix} $$

$$ {}^{1}_{2}T^{i} = \begin{bmatrix} c\theta_2^i & 0 & -s\theta_2^i & -d^i s\theta_2^i \\ s\theta_2^i & 0 & c\theta_2^i & d^i c\theta_2^i \\ 0 & -1 & 0 & 0 \\ 0 & 0 & 0 & 1 \end{bmatrix} $$

$$ {}^{2}_{3}T^{i} = \begin{bmatrix} c\theta_3^i & -s\theta_3^i & 0 & 0 \\ s\theta_3^i & c\theta_3^i & 0 & 0 \\ 0 & 0 & 1 & 0 \\ 0 & 0 & 0 & 1 \end{bmatrix} $$

$$ {}^{3}_{4}T^{i} = \begin{bmatrix} s\theta_4^i & c\theta_4^i & 0 & 0 \\ 0 & 0 & 1 & 0 \\ c\theta_4^i & -s\theta_4^i & 0 & 0 \\ 0 & 0 & 0 & 1 \end{bmatrix} {}^{4}_{5}T^{i} = \begin{bmatrix} 1 & 0 & 0 & L \\ 0 & 1 & 0 & 0 \\ 0 & 0 & 1 & 0 \\ 0 & 0 & 0 & 1 \end{bmatrix} $$

So, the total transformation matrix of frame B to frame 5 of link i can be written as: ${}^{B}_{5}T^{i} = {}^{B}_{1}T^{i}\,{}^{1}_{2}T^{i}\,{}^{2}_{3}T^{i}\,{}^{3}_{4}T^{i}\,{}^{4}_{5}T^{i}$ , or

$$ {}^{B}_{5}T^{i} = \begin{bmatrix} {}^{B}_{5}T^{i}_{1,1} & {}^{B}_{5}T^{i}_{1,2} & {}^{B}_{5}T^{i}_{1,3} & {}^{B}_{5}T^{i}_{1,4} \\ {}^{B}_{5}T^{i}_{2,1} & {}^{B}_{5}T^{i}_{2,2} & {}^{B}_{5}T^{i}_{2,3} & {}^{B}_{5}T^{i}_{2,4} \\ {}^{B}_{5}T^{i}_{3,1} & {}^{B}_{5}T^{i}_{3,2} & {}^{B}_{5}T^{i}_{3,3} & {}^{B}_{5}T^{i}_{3,4} \\ {}^{B}_{5}T^{i}_{4,1} & {}^{B}_{5}T^{i}_{4,2} & {}^{B}_{5}T^{i}_{4,3} & {}^{B}_{5}T^{i}_{4,4} \end{bmatrix} $$

(1) where

$$ {}^{B}_{5}T^{i}_{1,1} = \left(c\theta_1^i c\theta_2^i c\theta_3^i - s\theta_1^i s\theta_3^i\right) s\theta_4^i - c\theta_1^i s\theta_2^i c\theta_4^i $$

$$ {}^{B}_{5}T^{i}_{2,1} = \left(s\theta_1^i c\theta_2^i c\theta_3^i + c\theta_1^i s\theta_3^i\right) s\theta_4^i - s\theta_1^i s\theta_2^i c\theta_4^i $$

$$ {}^{B}_{5}T^{i}_{3,1} = s\theta_2^i c\theta_3^i s\theta_4^i + c\theta_2^i c\theta_1^i $$

$$ {}^{B}_{5}T^{i}_{4,1} = 0 $$

$$ {}^{B}_{5}T^{i}_{1,2} = \left(c\theta_1^i c\theta_2^i c\theta_3^i - s\theta_1^i s\theta_3^i\right) c\theta_4^i + c\theta_1^i s\theta_2^i s\theta_4^i $$

$$ {}^{B}_{5}T^{i}_{2,2} = \left(s\theta_1^i c\theta_2^i c\theta_3^i + c\theta_1^i s\theta_3^i\right) c\theta_4^i + s\theta_1^i s\theta_2^i s\theta_4^i $$

$$ {}^{B}_{5}T^{i}_{3,2} = s\theta_2^i c\theta_3^i c\theta_4^i - c\theta_2^i s\theta_4^i $$

$$ {}^{B}_{5}T^{i}_{4,2} = 0 $$

$$ {}^{B}_{5}T^{i}_{1,3} = -c\theta_1^i c\theta_2^i s\theta_3^i - s\theta_1^i c\theta_3^i $$

$$ {}^{B}_{5}T^{i}_{2,3} = -s\theta_1^i c\theta_2^i s\theta_3^i + c\theta_1^i c\theta_3^i $$

$$ {}^{B}_{5}T^{i}_{3,3} = -s\theta_2^i s\theta_3^i $$

$$ {}^{B}_{5}T^{i}_{4,3} = 0 $$

$$ {}^{B}_{5}T^{i}_{1,4} = \left(\left(c\theta_1^i c\theta_2^i c\theta_3^i - s\theta_1^i s\theta_3^i\right) s\theta_4^i - c\theta_1^i s\theta_2^i c\theta_4^i\right) L - d^i \left(c\theta_1^i s\theta_2^i\right) + r_b c\theta_1^i $$

$$ {}^{B}_{5}T^{i}_{2,4} = \left(\left(s\theta_1^i c\theta_2^i c\theta_3^i + c\theta_1^i s\theta_3^i\right) s\theta_4^i - s\theta_1^i s\theta_2^i c\theta_4^i\right) L - d^i \left(s\theta_1^i s\theta_2^i\right) + r_b s\theta_1^i $$

$$ {}^{B}_{5}T^{i}_{3,4} = \left(s\theta_2^i c\theta_3^i s\theta_4^i + c\theta_2^i c\theta_4^i\right) L + d^i \left(c\theta_2^i\right) $$

$$ {}^{B}_{5}T^{i}_{4,4} = 1 $$

We install 9 encoders instead of 6 encoders (an encoder for each actuator). The additional 3 encoders are for measuring the

$\theta_4^1, \theta_1^2, \theta_4^3$. So, the origin of coordinate frame 5 for link i with respect to coordinate frame B can be written as:

$$\begin{bmatrix} {}^{B}_{5}\vec{P}^{i} \\ 1 \end{bmatrix} = {}^{B}_{5}T^{i} \times \begin{bmatrix} 0 \\ 0 \\ 0 \\ 1 \end{bmatrix}$$

$$= \begin{bmatrix} \left(\left(c\theta_1^i c\theta_2^i c\theta_3^i - s\theta_1^i s\theta_3^i\right)s\theta_4^i - c\theta_1^i s\theta_2^i c\theta_4^i\right)L \\ \quad - d^i\left(c\theta_1^i s\theta_2^i\right) + r_b c\theta_1^i \\ \left(\left(s\theta_1^i c\theta_2^i c\theta_3^i + c\theta_1^i s\theta_3^i\right)s\theta_4^i - s\theta_1^i s\theta_2^i c\theta_4^i\right)L \\ \quad - d^i\left(s\theta_1^i s\theta_2^i\right) + r_b s\theta_1^i \\ \left(s\theta_2^i c\theta_3^i s\theta_4^i + c\theta_2^i c\theta_4^i\right)L + d^i\left(c\theta_2^i\right) \\ 1 \end{bmatrix}$$

Figure 2 shows the vector which locates the origin of the upper frame with respect to the origin of the base frame and the corresponding homogeneous transformation can be written as:

${}^{B}_{M}T = \begin{bmatrix} \vec{n} & \vec{o} & \vec{a} & {}^{B}_{M}\vec{P} \\ 0 & 0 & 0 & 1 \end{bmatrix}$ where the position vector is

$${}^{B}_{M}\vec{P} = \frac{1}{3}\left({}^{B}_{5}\vec{P}^{1} + {}^{B}_{5}\vec{P}^{2} + {}^{B}_{5}\vec{P}^{3}\right)$$

The Orientation of frame M with respect to frame B is:

$$\vec{n} = \frac{{}^{B}_{5}\vec{P}^{1} - {}^{B}_{M}\vec{P}}{\left|{}^{B}_{5}\vec{P}^{1} - {}^{B}_{M}\vec{P}\right|},\ \vec{o} = \frac{{}^{B}_{5}\vec{P}^{2} - {}^{B}_{5}\vec{P}^{3}}{\left|{}^{B}_{5}\vec{P}^{2} - {}^{B}_{5}\vec{P}^{3}\right|},\ \vec{a} = \vec{n} \times \vec{o}$$

## Inverse Kinematics

Figure 4 defined the position vectors needed for the inverse kinematics as follows:

Position vector $\vec{P} = \begin{bmatrix} X & Y & Z \end{bmatrix}^T$ represents the vector which locates the origin of the upper frame ($O_M$) with respect to the origin of the base ($O_B$). For link i,

$$\vec{r}_m^{\,i} = \begin{bmatrix} r_m c\theta_1^i & r_m s\theta_1^i & 0 \end{bmatrix}^T,$$

$$\vec{r}_b^{\,i} = \begin{bmatrix} r_b c\theta_1^i & r_b s\theta_1^i & 0 \end{bmatrix}^T,$$

Where $\theta_1^1 = 0^o, \theta_1^2 = 120^o, \theta_1^3 = 240^o$

If $d^i$ = distance of sliding joint from origin, then, intuitively, the vector from the base of each link to the sliding joint in the base coordinate system can be written as:

$$\vec{d}^{\,i} = \begin{bmatrix} d_x^i & d_y^i & d_z^i \end{bmatrix}^T = D^i \vec{d}_u^{\,i} \text{ where}$$

$$D^i = \begin{bmatrix} d^i & 0 & 0 \\ 0 & d^i & 0 \\ 0 & 0 & d^i \end{bmatrix} \text{ and}$$

$\vec{d}_u^{\,i} = \begin{bmatrix} -c\theta_1^i s\theta_2^i & -s\theta_1^i s\theta_2^i & c\theta_2^i \end{bmatrix}^T$ (represents the unit vector of $\vec{d}^{\,i}$).

L is the link length as shown in Figure 3, or

$\vec{L}^i = \begin{bmatrix} L_x^i & L_y^i & L_z^i \end{bmatrix}^T$ represents the vector of link $i$.

The desired joint variables, $\theta_3^i$, $\theta_1^i$, $d^i$, can be derived from the equation below:

$$\vec{B}^i = \vec{P} + {}^{B}_{M}R\vec{r}_m^{\,i} - \vec{r}_b^{\,i}$$

$${}^{B}_{5}\vec{P}^{\,i} = \vec{P} + {}^{B}_{M}R\vec{r}_m^{\,i} = {}^{B}_{M}T\vec{r}_m^{\,i}$$

so, $\vec{B}^i = {}^{B}_{M}T\vec{r}_m^{\,i} - \vec{r}_b^{\,i}$, where

${}^{B}_{M}R = \begin{bmatrix} \vec{n} & \vec{o} & \vec{a} \end{bmatrix} = R_{RPY}$ represent the Roll-Pitch-Yaw orientation, $R_{RPY}$, which is equal to:

$$R_{RPY} = \begin{bmatrix} c\alpha c\beta & c\alpha s\beta s\gamma - s\alpha c\gamma & c\alpha s\beta c\gamma + s\alpha s\gamma \\ s\alpha c\beta & s\alpha s\beta s\gamma + c\alpha c\gamma & s\alpha s\beta c\gamma - c\alpha s\gamma \\ -s\beta & c\beta s\gamma & c\beta c\gamma \end{bmatrix}$$

where $\alpha$ = Roll, $\beta$ = Pitch, $\gamma$ = Yaw. These Euler angles will used as orientation command for the slave-arm as shown in Figure 7

So, $\vec{B}^i$ is equal to:

$$\begin{bmatrix} \vec{B}^i \\ 1 \end{bmatrix} = \begin{bmatrix} B_x^i \\ B_y^i \\ B_z^i \\ 1 \end{bmatrix} = {}^{B}_{M}T \begin{bmatrix} r_m c\theta_1^i \\ r_m s\theta_1^i \\ 0 \\ 1 \end{bmatrix} - \begin{bmatrix} r_b c\theta_1^i \\ r_b s\theta_1^i \\ 0 \\ 1 \end{bmatrix}$$

where ${}^{B}_{M}T$ is derived previously, so $B_x^i, B_y^i, B_z^i$ can be written as:

$$B_x^i = \left(\left(c\theta_1^i c\theta_2^i c\theta_3^i - s\theta_1^i s\theta_3^i\right)s\theta_4^i - c\theta_1^i s\theta_2^i c\theta_4^i\right)L - d^i\left(c\theta_1^i s\theta_2^i\right) \quad (2)$$

$$B_y^i = \left(\left(s\theta_1^i c\theta_2^i c\theta_3^i + c\theta_1^i s\theta_3^i\right)s\theta_4^i - s\theta_1^i s\theta_2^i c\theta_4^i\right)L - d^i\left(s\theta_1^i s\theta_2^i\right) \quad (3)$$

$$B_z^i = \left(s\theta_2^i c\theta_3^i s\theta_1^i + c\theta_2^i c\theta_4^i\right)L + d^i\left(c\theta_2^i\right) \quad (4)$$

Equations (2) – (4) are used for solving $\theta_3^i$ by multiplying both sides of equation (3) and (4) with $c\theta_2^i$ and $s\theta_1^i s\theta_2^i$, respectively. Then, adding them together to eliminate $d^i$, we will obtain:

$$s\theta_1^i s\theta_2^i B_z^i + c\theta_2^i B_y^i = \left(s\theta_1^i c\theta_3^i + c\theta_1^i c\theta_2^i s\theta_3^i\right)s\theta_4^i L$$

So, $$s\theta_4^i L = \frac{s\theta_1^i s\theta_2^i B_z^i + c\theta_2^i B_y^i}{s\theta_1^i c\theta_3^i + c\theta_1^i c\theta_2^i s\theta_3^i} \quad (5)$$

Similarly, multipling both sides of equation (2) and (4) with $c\theta_2^i$ and $c\theta_1^i s\theta_2^i$ respectively, then suming them together, we will obtain:

$$c\theta_1^i s\theta_2^i B_z^i + c\theta_2^i B_x^i = \left(c\theta_1^i c\theta_3^i - s\theta_1^i c\theta_2^i s\theta_3^i\right) s\theta_4^i L$$

So, $$s\theta_4^i L = \frac{c\theta_1^i s\theta_2^i B_z^i + c\theta_2^i B_x^i}{c\theta_1^i c\theta_3^i - s\theta_1^i c\theta_2^i s\theta_3^i} \quad (6)$$

From equation (5) and (6), $\theta_3^i$ can be obtained as follows:

$$\theta_3^i = \arctan\left(\frac{c\theta_1^i c\theta_2^i B_y^i - s\theta_1^i c\theta_2^i B_x^i}{c\theta_2^i s\theta_2^i B_z^i + \left(c\theta_2^i\right)^2\left(c\theta_1^i B_x^i + s\theta_1^i B_y^i\right)}\right) \quad (7)$$

Similarly, it can be shown that:

$$\theta_4^i = \arcsin\left(\frac{s\theta_2^i B_z^i + c\theta_2^i\left(c\theta_1^i B_x^i + s\theta_1^i B_y^i\right)}{c\theta_3^i L}\right) \quad (8)$$

with a condition that:

$$\left|c\theta_3^i L\right| \geq \left|\frac{s\theta_2^i B_z^i + c\theta_2^i\left(c\theta_1^i B_x^i + s\theta_1^i B_y^i\right)}{c\theta_3^i L}\right|$$

Our design $\theta_4^i \leq 50^0$

And $d^i$ can be derived from equation (4) as:

$$B_z^i = \left(s\theta_2^i c\theta_3^i s\theta_1^i + c\theta_2^i c\theta_4^i\right) L + d^i\left(c\theta_2^i\right)$$

So, $$d^i = \frac{B_z^i - \left(s\theta_2^i c\theta_3^i s\theta_4^i + c\theta_2^i c\theta_4^i\right) L}{c\theta_2^i} \quad (9)$$

**Jacobian**

The Jacobian is the relationship between the twist velocity of the moving platform and the velocity of the joint variables, where the actuators are attached. From the relationship $Bt = A\dot{q}$, where the matrix $A$, $B$ are the Jacobian matrix of the closed-loop chain and:

$t = \begin{bmatrix}\omega \\ v\end{bmatrix} = \begin{bmatrix}\omega_x & \omega_y & \omega_z & v_x & v_y & v_z\end{bmatrix}^T$ represents the velocity of the top plate which consists of the angular velocity $(\omega)$ and linear velocity $(v)$.

$\dot{q} = \begin{bmatrix}\dot{d}^1 & \dot{\theta}_3^1 & \dot{d}^2 & \dot{\theta}_3^2 & \dot{d}^3 & \dot{\theta}_3^3\end{bmatrix}^T$ represents the velocity of the joint variables where the actuators are attached.

From figure 5, the velocity of point $P_j$ is:

$$\dot{\vec{P}}_j = \dot{d}\vec{S}_{j1} + \dot{\theta}_3\vec{S}_{j2} + \dot{\theta}_4\vec{S}_{j3} \quad (10)$$

Or $$\dot{\vec{P}}_j = \vec{v} - \vec{\omega}\times\vec{r}_{mj} \quad (11)$$

where

$\vec{S}_{j1} = \vec{e}_j$, $\vec{S}_{j2} = \vec{f}_j \times \vec{r}_{fj}$, $\vec{S}_{j3} = \vec{g}_j \times \vec{r}_{qj}$,

$\vec{r}_{mj} = \vec{P} - \vec{P}_j$

$\vec{r}_{fj} = \vec{r}_{qj} = \vec{P}_j - {}^B_4\vec{P}_j = \vec{P}_j - {}^B_3\vec{P}_j$

$$\vec{r}_{fj} = L\begin{bmatrix}\left(c\theta_1 c\theta_2 c\theta_3 - s\theta_1 s\theta_3\right) s\theta_4 - c\theta_1 s\theta_2 c\theta_4 \\ \left(s\theta_1 c\theta_2 c\theta_3 + c\theta_1 s\theta_3\right) s\theta_4 - s\theta_1 s\theta_2 c\theta_4 \\ s\theta_2 c\theta_3 s\theta_4 + c\theta_2 c\theta_4\end{bmatrix}$$

$j = 1,2,3$

And because:

$$\left(\vec{S}_{j2}\times\vec{S}_{j3}\right)^T\cdot\dot{\vec{P}}_j = \dot{d}\left(\vec{S}_{j2}\times\vec{S}_{j3}\right)^T\cdot\vec{S}_{j1} \quad (12)$$

So,

$$\frac{\left(\vec{S}_{j2}\times\vec{S}_{j3}\right)^T}{\left|\vec{S}_{j2}\times\vec{S}_{j3}\right|}\cdot\dot{\vec{P}}_j = \dot{d}\frac{\left(\vec{S}_{j2}\times\vec{S}_{j3}\right)^T\cdot\vec{S}_{j1}}{\left|\vec{S}_{j2}\times\vec{S}_{j3}\right|} \quad (13)$$

Given:

$J_j = \begin{bmatrix}\vec{S}_{j1} & \vec{S}_{j2} & \vec{S}_{j3}\end{bmatrix}$ has dimension 3x3

$\Delta_j = \det(J_j) = \left(\vec{S}_{j1}\times\vec{S}_{j2}\right)^T\cdot\vec{S}_{j3}$ . So,

$\Delta_j = -s_{j4}c_{j4}L^2$ and:

$a_{j1} = \frac{\Delta_j}{\left|\vec{S}_{j2}\times\vec{S}_{j3}\right|}$ (dimension 1x1). So,

$a_{j1} = -c_{j4}$

$\vec{I}_j = \frac{\vec{S}_{j2}\times\vec{S}_{j3}}{\left|\vec{S}_{j2}\times\vec{S}_{j3}\right|}$ is the unit vector parallel to the vector of $\left(\vec{S}_{j2}\times\vec{S}_{j3}\right)$. So,

$$\vec{I}_j = \begin{bmatrix}\left(s\theta_1 s\theta_3 - c\theta_1 c\theta_2 c\theta_3\right) s\theta_1 + c\theta_1 s\theta_2 c\theta_4 \\ -\left(c\theta_1 s\theta_3 + s\theta_1 c\theta_2 c\theta_3\right) s\theta_4 + s\theta_1 s\theta_2 c\theta_1 \\ -\left(s\theta_2 c\theta_3 s\theta_4 + c\theta_2 c\theta_1\right)\end{bmatrix}_j$$

From the above equation with equation (11) and equation (13), we will obtain:

$$a_{j1}\cdot\dot{d} = \vec{I}_j\cdot\left(\vec{v} - \vec{\omega}\times\vec{r}_{mj}\right) \quad (14)$$

Given $b_{j1} = \begin{bmatrix}\left(\vec{I}_j\times\vec{r}_{mj}\right)^T & \vec{I}_j^T\end{bmatrix}$ (dimension 1x6).

So, from equation (14), we will obtain:

$$a_{j1}\cdot\dot{d} = b_{j1}t \quad (15)$$

From equation (10), we will obtain:

$$\left(\vec{S}_{j3}\times\vec{S}_{j1}\right)^T\cdot\dot{\vec{P}}_j = \dot{\theta}_{3j}\left(\vec{S}_{j3}\times\vec{S}_{j1}\right)^T\cdot\vec{S}_{j2} \quad (16)$$

So, $$\frac{\left(\vec{S}_{j3}\times\vec{S}_{j1}\right)^T}{\left|\vec{S}_{j3}\times\vec{S}_{j1}\right|}\cdot\dot{\vec{P}}_j = \dot{\theta}_{3j}\frac{\left(\vec{S}_{j3}\times\vec{S}_{j1}\right)^T\cdot\vec{S}_{j2}}{\left|\vec{S}_{j3}\times\vec{S}_{j1}\right|} \quad (17)$$

Given $a_{j2} = \frac{\Delta_j}{\left|\vec{S}_{j3}\times\vec{S}_{j1}\right|}$ (dimension 1x1)

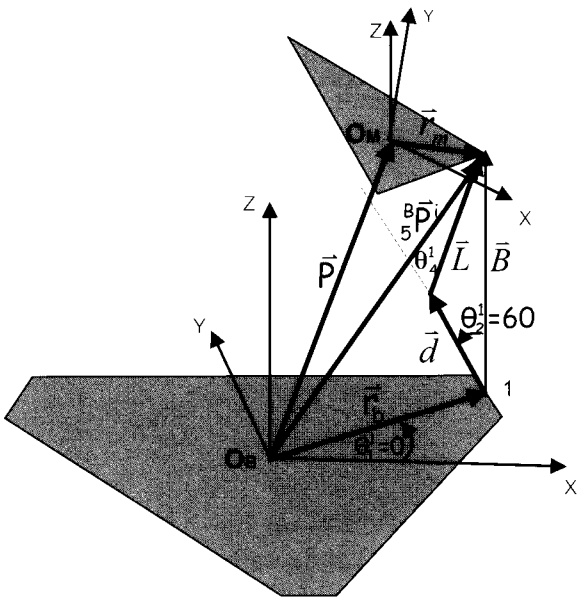


**Figure 4.** The necessary vectors needed for deriving invert kinematics.

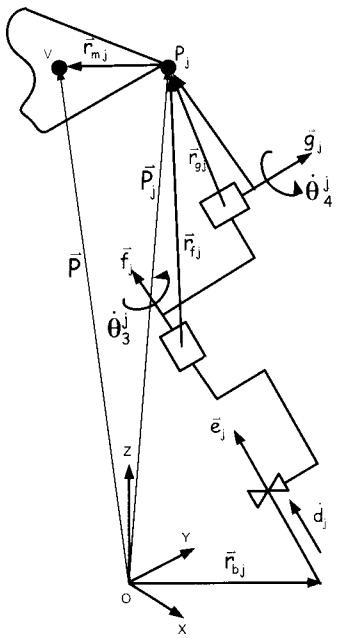


**Figure 5.** The position vector of link j

So, $a_{j2} = -s_{j4}L$ $\vec{M}_j = \dfrac{\vec{S}_{j3} \times \vec{S}_{j1}}{\left|\vec{S}_{j3} \times \vec{S}_{j1}\right|}$ is the unit vector parallel to the vector of $\left(\vec{S}_{j3} \times \vec{S}_{j1}\right)$. So,

$$\vec{M}_j = \begin{bmatrix} c\theta_1 c\theta_2 s\theta_3 + s\theta_1 c\theta_3 \\ s\theta_1 c\theta_2 s\theta_3 - c\theta_1 c\theta_3 \\ s\theta_2 s\theta_3 \end{bmatrix}$$

From the above equation with equation (11) and equation (17), we will obtain:

$$a_{j2} \cdot \dot{\theta}_{3j} = \vec{M}_j \cdot \left(\vec{v} - \vec{\omega} \times \vec{r}_{mj}\right) \qquad (18)$$

Given $b_{j2} = \left[\left(\vec{M}_j \times \vec{r}_{mj}\right)^T \quad \vec{M}_j^T\right]$ (dimension 1x6). So, from equation (18), we obtain:

$$a_{j2} \cdot \dot{\theta}_{3j} = b_{j2} t$$

So, the matrix A can be written as

$$A = \begin{bmatrix} a_{11} & 0 & 0 & 0 & 0 & 0 \\ 0 & a_{12} & 0 & 0 & 0 & 0 \\ 0 & 0 & a_{21} & 0 & 0 & 0 \\ 0 & 0 & 0 & a_{22} & 0 & 0 \\ 0 & 0 & 0 & 0 & a_{31} & 0 \\ 0 & 0 & 0 & 0 & 0 & a_{32} \end{bmatrix}$$

which is a diagonal matrix. So, $A^{-1}$ can be obtained from

$$A^{-1} = \begin{bmatrix} 1/a_{11} & 0 & 0 & 0 & 0 & 0 \\ 0 & 1/a_{12} & 0 & 0 & 0 & 0 \\ 0 & 0 & 1/a_{21} & 0 & 0 & 0 \\ 0 & 0 & 0 & 1/a_{22} & 0 & 0 \\ 0 & 0 & 0 & 0 & 1/a_{31} & 0 \\ 0 & 0 & 0 & 0 & 0 & 1/a_{32} \end{bmatrix}$$

And the matrix B is equal to:

$$B = \begin{bmatrix} b_{11} \\ b_{12} \\ b_{21} \\ b_{22} \\ b_{31} \\ b_{32} \end{bmatrix} = \begin{bmatrix} \left(\vec{I}_1 \times \vec{r}_{m1}\right)^T & \vec{I}_1^T \\ \left(\vec{M}_1 \times \vec{r}_{m1}\right)^T & \vec{M}_1^T \\ \left(\vec{I}_2 \times \vec{r}_{m2}\right)^T & \vec{I}_2^T \\ \left(\vec{M}_2 \times \vec{r}_{m2}\right)^T & \vec{M}_2^T \\ \left(\vec{I}_3 \times \vec{r}_{m3}\right)^T & \vec{I}_3^T \\ \left(\vec{M}_3 \times \vec{r}_{m3}\right)^T & \vec{M}_3^T \end{bmatrix}$$

The relationship of the force at the endpoint of the haptic system and the joint torque for the parallel mechanism can be written as:

$$F = J^T \tau,$$

where $F = \begin{bmatrix} M_x & M_y & M_z & F_x & F_y & F_z \end{bmatrix}^T$ is the Moment (M) and force (F) applied at the endpoint (top plate) of the haptic device.

$\tau = \begin{bmatrix} f_1 & \tau_1 & f_2 & \tau_2 & f_3 & \tau_3 \end{bmatrix}^T$ is the joint torque of the actuators where $f$ and $\tau$ are the force at the prismatic or sliding joint $\left(d^i\right)$ and torque of the revolute joint $\left(\theta_3^i\right)$,

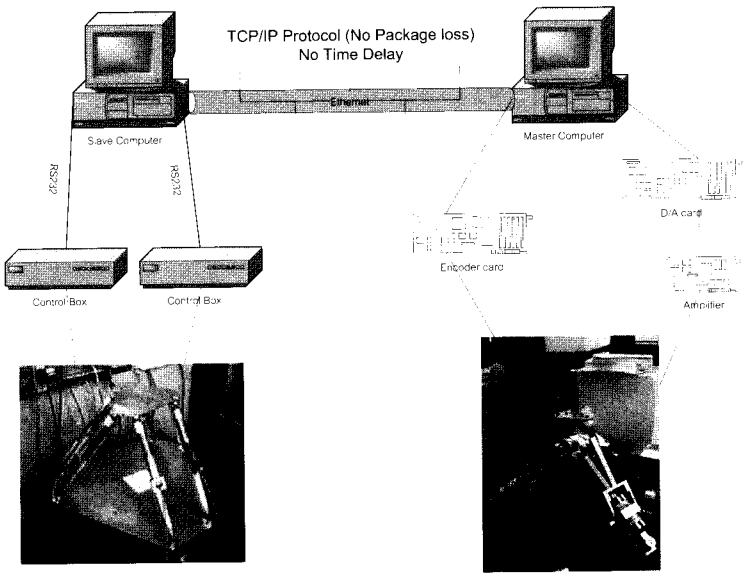


**Figure 6.** The connection between the master-arm (haptic) and the slave-arm (Stewart)

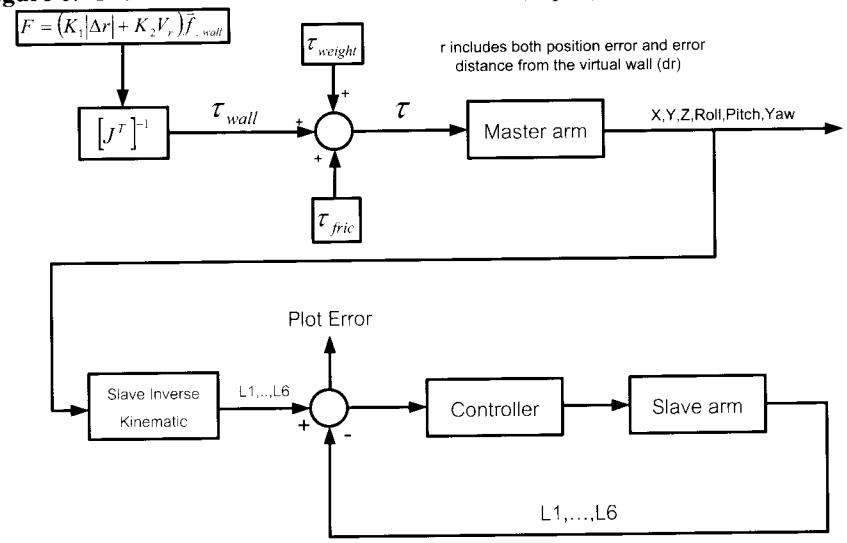


**Figure 7** The structure of the control system.

respectively. So, the Jacobian matrix is $J = A^{-1}B$. The singularity of the system will occur when $\det(A) = 0$ or $\det(B) = 0$ or $\det(A^{-1}B) = 0$. It can be shown that, for the proposed mechanism, there is no singularity.

## 3. The Controller

Figure 6 shows the connection between the master-arm or the haptic system and the slave-arm (the Stewart platform) [1] through our intranet network using TCP/IP protocol. Due to the slow update time, we assume that there is no effect from package lose and time delay. The sampling time of the master-arm is faster than the sampling time of the slave-arm and these are set independently. The slave-arm requests commands from the master-arm, So that both arms do not need to start at the same time. The endpoint position and orientation of the haptic system will be transformed to the joint command of the Stewart platform. The controller handles both position control and force control.

Figure 7 is the diagram to show the master-slave control system. The operator will control or maneuver the master arm though the control stick. The virtual wall (will be explained in next section) will be specified in advance, if necessary, to specify the boundary or work

space. When the control stick hits the virtual wall, the reaction force F, which will react to the operator, will be generated by the controller in the Cartesian space of the haptic system. The reaction force consists of 2 components, the force normal to the virtual wall and the viscous force generated by the controller to prevent the control stick moving to fast. The reaction force F, in Cartesian space, can be transformed into the joint space by using the Jacobian matrix. The friction force compensation is also included in the control system as shown in Figure 7. When the control stick is inside the working area or in the free area, the reaction force applied at the control stick will only consist of the viscous force and friction compensation force. The information from the encoders at each joint of the master arm will be used to calculate the desired path motion, translation and orientation, of the slave. The details of the kinematics of the slave arm can be consulted from [1]. Then the joint variables of each link of the slave arm can be calculated by using inverse kinematics. The PID control is used in the control loop of the slave arm as shown in Figure 7. Then, the position and orientation error of the slave arm are obtained from the comparison of the measurement values with the input or the reference values.

## 4. Virtual Wall

The concept of virtual wall is to specify the working area of the master arm virtually. This will help the operator to work conveniently in the specific area. Figure 8 shows the circular working area. The virtual wall is defined by a function, f(x,y,z) = constant. When the operator move the master arm contact to the virtual wall, the reaction force, F, will be generated against the operation motion.

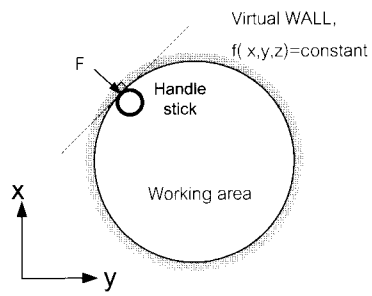


**Figure 8.** The circular working area

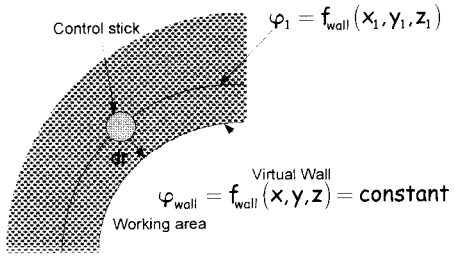


**Figure 9.**The control stick is beyond the virtual wall

From Figure 9, the force F can be evaluated from:

$$F = (K_1 dr)\ \vec{n} + (K_2 V)\vec{n}$$

where

$dr = \dfrac{d\varphi|\nabla\varphi|}{\nabla\varphi \cdot \nabla\varphi}$ = the distance between the control stick and the virtual wall

$\vec{n} = \pm\dfrac{\nabla\varphi}{|\nabla\varphi|}$ = the unit normal vector to the virtual wall

$$\nabla\varphi = \mathrm{i}\frac{\partial\varphi}{\partial x} + j\frac{\partial\varphi}{\partial y} + k\frac{\partial\varphi}{\partial z}$$

$V$ = velocity of the control stick

$(K_1 dr)\ \vec{n}$ = reaction force normal to the wall

$(K_2 V)\vec{n}$ = viscous force generated by the controller

$K_1$, $K_2$ = amplifier gains

So, the force F can be written as:

$$F = \frac{K_1 d\varphi}{|\nabla\varphi|^2}\nabla\varphi + K_2 V\frac{\nabla\varphi}{|\nabla\varphi|} \quad \text{where}$$

$$d\varphi = f_{wall}(x_1, y_1, z_1) - f_{wall}(x, y, z)$$
$$= f_{wall}(x_1, y_1, z_1) - \varphi_{wall}$$
$$= f_{wall}(x_1, y_1, z_1) - constant$$

## 5. Experimental Results

Table 1 shows the maximum error measured at the endpoint of the Stewart platform. The experiment is done with 300 Hz, sampling frequency, for the haptic system and 20 Hz for the Stewart platform. The sampling frequencies are limited due to the hardware capability. The error will be significantly reduced by increasing the sampling frequencies.

Figures 10 and 11 are the 3D and 2D diagram, respectively, of the endpoint position of the haptic arm with circular virtual wall. The center point of the circular virtual wall is at x,y,z = 0. From Figure 11, we can estimate that the error from the virtual wall is approximately 4 mm. This is due to the limitation of the

controller hardware of the haptic system and the Stewart platform. This error can be improved if we can increase the sampling frequencies of both the haptic system and the Stewart platform. Otherwise the digital controller design technique is needed for studying the sampling time effect to the controlled system. The reaction force from the virtual wall is also illustrated in the figure.

The haptic arm can be performed as a slave arm as well. We develop a computer graphic program to test the capability. As shown in Figure 12, the computer graphic program consists of an airplane which can be programmed to fly automatically or controlled by the haptic arm. The position and orientation of the airplane will be converted to the position and orientation command for the haptic arm and vice versa. For the case of haptic arm controlled by the airplane, by applying inverse kinematics, the links command of the haptic arm are generated and used as control parameters of the haptic arm controller. Figure 12 shows an example of some instants of the motion.

| Link i | Error (mm) |
|---|---|
| 1 | 2.07 |
| 2 | 3.85 |
| 3 | 1.34 |
| 4 | 1.08 |
| 5 | 1.51 |
| 6 | 2.52 |

**Table 1.** The maximum error of the endpoint (top plate) of the Stewart Platform

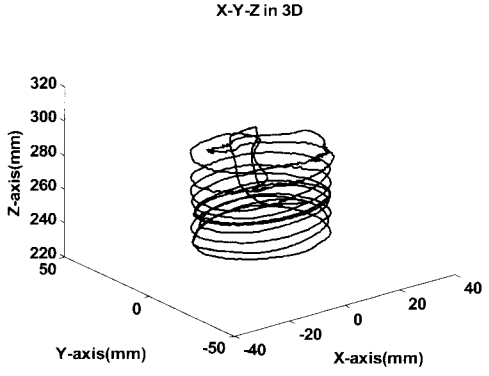


**Figure 10.** The 3D diagram of the endpoint of the haptic arm with circular virtual wall (cylindrical volume)

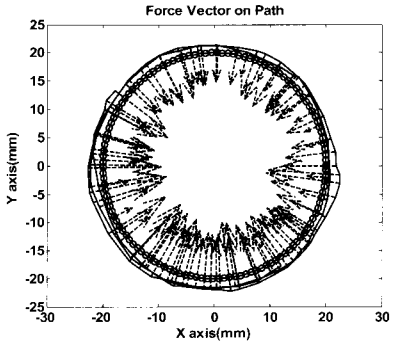


_____ Endpoint position of the haptic Arm
-o-o-o- Circular virtual wall, → force reaction from virtual wall

**Figure 11.** The 2D diagram of the endpoint of the haptic arm with circular virtual wall

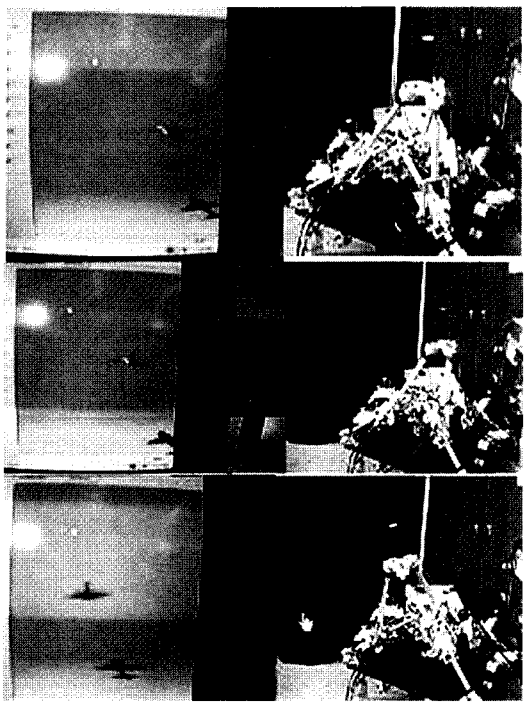

**Figure 12** example shows the haptic arm performing as a slave arm

## 6. Conclusion

This work concerns the design and development of a six degrees of freedom haptic device. The inverse and forward kinematics as well as the Jacobian are derived. Instead of 6 encoders, we installed 9 encoders to help to

obtain the forward kinematics, especially in closed-form format, which is normally difficult for parallel mechanisms. We also show that this mechanism is singularity free. We introduce the concept of virtual wall to better specify working areas. The experimental results show that the haptic device is capable of controlling the Stewart platform. Intuitively, it can be used for other parallel mechanisms as well.

## 7. References


[1] *Viboon Sangveraphunsiri, Prasartporn Wongkumchang,* Design and Control of a Stewart Platform, the 15th National Conference of Mechanical Engineering, 2001, (in Thai).

[2] *Viboon Sangveraphunsiri, Tawee, Ngamvilaikorn.* Design and Development of a Six DOF Master-Slave Human-Assisted Manipulator Arm, 2002 JSAE Annual Congress, Yokohama, Japan, July, 2002.

[3] *Viboon Sangveraphunsiri and Thitipon satthaporn,* Internet-Based Teleoperation Using the WWW, 1999 Asian Machine Tool, November 1999, Thailand.

[4] *Sangveraphunsiri, V. and Tantawiroon, N.* Novel Design of a 4 DOF Parallel Robot., 2003 JSAE Annual Congress, Yokohama, Japan, May 21 – 23, 2003.

[5] *Ki Young Woo, Byoung Dae Jin and Dong-Soo Kwon,* A 6-DOF Force-Reflecting Hand Controller Using the Fivebar Parallel Mechanism, Proceedings of the 1998 IEEE International Conference on Robotics & Automation, Leuven, Belgium, May 1998, pp. 1597-1602.

[6] *Xiaolun Shi and R.G. Fenton,* A Complete and General Solution to the Forward Kinematics Problem of Platform-Type Robotic Manipulators, Proceedings of the 1994 IEEE International Conference on Robotics & Automation, 1994, pp. 3055-3062.

[7] *Jungwon Yoon and Jeha Ryu,* Control and Evaluation of a New 6-DOF Haptic Device Using a Parallel Mechanism, Proceedings of the 2000 IEEE/RSJ International Conference on Intelligent Robots and Systems, 2000, pp. 1125-1130.

[8] *Alain Tremblay and Luc Baron,* Geometrical Synthesis of Star-Like Topology Parallel Manipulators with a Genetic Algorithm, Proceedings of the 1999 IEEE International Conference on Robotics & Automation, Detroit, Michigan, May 1999, pp. 2446-2451.

[9] *Clement M. Gosselin and Jean-Francois Hamel,* The Agile Eye: a High-performance three-degree-of-freedom Camera-orienting Device. Proceedings of the 1994 IEEE International Conference on Robotics & Automation, pp. 781-786, 1994.